

# Synthesis of Pure and High Surface Area Sodalite Catalyst from Waste Industrial Brine and Coal Fly Ash for Conversion of Waste Cooking Oil (WCO) to Biodiesel

T.C. Aniokete, M. Ozonoh, and M.O. Daramola<sup>‡</sup>

School of Chemical and Metallurgical Engineering, Faculty of Engineering and the Built Environment, University of the Witwatersrand, Wits 2050, Johannesburg, South Africa

([t.c.anioke@live.com](mailto:t.c.anioke@live.com); [maxwellba@yahoo.com](mailto:maxwellba@yahoo.com); [michael.daramola@wits.ac.za](mailto:michael.daramola@wits.ac.za))

<sup>‡</sup> Corresponding Author, Tel.: +27117177536; [michael.daramola@wits.ac.za](mailto:michael.daramola@wits.ac.za)

*Received: 17.07.2019 Accepted: 06.10.2019*

**Abstract-** Recently, the devastating environmental threat of coal usage in power generation and high biodiesel production costs had led to worldwide energy discourse. The cost of producing and thus economical and environmentally sustainable use of biodiesel could be reduced by non-waste derived heterogeneous catalysts prepared from waste products. In this preliminary study, coal fly ash and industrial waste brine of South African origin were valorized for the synthesis of waste-derived solid hydroxy sodalite (HSOD) catalyst. Catalysts derived from non-waste are not sustainable economically and environmentally. However, the method of hydrothermal synthesis was used to synthesize the catalysts used in a batch reactor to produce biodiesel. The catalyst's physicochemical characteristics were studied using X-ray diffraction, Scanning electron microscopy and Fourier transform infrared. The catalyst's textural property was acquired at 77K through nitrogen physisorption using Brunauer-Emmett-Teller (BET) technique. The catalyst was subjected to performance evaluation to produce biodiesel from waste cooking oil under the following reaction conditions: 15:1 methanol-to-waste cooking oil ratio, 3 wt percent of catalysts, 300-500 r.p.m. agitation speed, 8 h reaction time and 60 °C temperature. The biodiesel yield for the waste catalyst and the non-waste catalyst was 89.4 and 85.0 percent respectively, with a peak conversion of 97.0 percent of the waste cooking oil. BET analytical results indicate that the surface area of waste derived and non-waste derived catalysts was respectively 33.05 m<sup>2</sup>g<sup>-1</sup> and 0.1645 m<sup>2</sup>g<sup>-1</sup>.

**Keywords:** Coal Fly Ash; Biodiesel; Waste Industrial Brine; Hydroxy Sodalite Catalyst; Waste Cooking Oil.

## 1. Introduction

South Africa as a notable stakeholder in the Sub-Saharan African continent largely depends on Eskom's coal-combusted electricity generation to drive her economy. The exploitation of coal fossil fuel is sustainable due to its abundance in the land. Cheap source of coal in the country has been a chief source of 93 % of the nation's electricity supply [1] required for energizing the nation's massive infrastructure, industrialization stride, socioeconomic sustenance [2,3] and accelerated population growth [4]. However, it is warned that this risky dependence on coal fossil resource utilization in the country and other Sub-Saharan states, has two key sources of environmentally unfriendly disposal impacts.

In one hand, the coal minefields potentially release waste industrial brine (WIB) into the open-landfill to the tune of 4.2 million tons annually in South Africa and on the other

hand, by combustion of approximately 120 million tons of coal, around 25 million tons of coal fly ash (CFA) were released into the ash or slurry dams, lakes or ponds every year [1].

The rising CFA dump and WIB discharge into the environment have attracted global attention to the occasion of urgent disposal management due to the negative threat these wastes pose to the health and quality of citizen's life and also a detriment to the green environment [5]. The country has been rated the largest emitter of carbon dioxide (CO<sub>2</sub>) in Sub-Saharan Africa and 12<sup>th</sup> in the world [6] due to sizzling concerns from citizens and other pressure groups against the environmental impact of industrial utilization of coal for energy generation. Notwithstanding the palliative measures of the World Bank project on CO<sub>2</sub> capture and storage (CCS) and the introduction of CO<sub>2</sub> tax reduction in the country, the Sub-Saharan African region is still ranked most vulnerable in the continent.

Therefore, there is a pertinent need to evolve an environmentally friendly approach to the utilization of the waste which is of urgent concern in terms of its disposal and management. In compliance with South Africa's waste management strategies, Eskom had embarked on a conservative measure to rehabilitate ash disposal sites through revegetation programs whereby fertile soils are used to cover the ashes and trees planted on them to minimize its negative environmental impact.

However, these approaches are temporary, cost-intensive and unsustainable, primarily due to the large volume of ash deposit which increases at geometrical proportions as more coal is combusted to meet the increasing energy [7] for technological development, socioeconomic and population pressures. Invariably, funds available to cope with disposal management issues such as the environmental, health and economic risks are limited.

Elsewhere [9,10], coal fly ash had been sold for industrial applications such as cement/concrete, lime pozzolanic, landfills, highways and embankments. Approximately 1.2 million tons of coal fly ashes are marketed in South Africa out of 25 million tons of coal fly ashes produced annually, among others, to cement industry where the ashes are used as cement extender.

The under-utilization of about 23.8 million tons of coal fly ash remains a huge management problem and with the existing number of coal combustion plants in South Africa, disposal of coal fly ashes and WIB has potential to contaminate underground water [10] through chemical seepage or leaching from ash dams, heaps/mounds or ponds in the case of CFA. Currently, much research efforts are focused on the development of eco-friendly, cost-effective and efficient technologies in the utilization of CFA and WIB as a beneficial disposal management approach to convert these wastes to high value-added zeolitic solid catalytic materials and other applications such as ion-exchange materials, adsorbents and molecular sieves.

Recently, CFA and WIB have been successfully converted hydrothermally to solid hydroxy sodalite adsorbent material [11]. Direct chemical synthesis of heterogeneous solid catalysts had been successful using the hydrothermal technique [12]. [12-14] described hydrothermal synthesis technique as an efficient and effective approach to the preparation of high-purity bulk metal catalysts, as the method proved to be cost-effective and easy to control in terms of its synthesis temperature and reaction time. Through hydrothermal technique, [14] synthesized hydroxy sodalite from pure chemical precursors with a BET surface area  $0.1643 \text{ m}^2\text{g}^{-1}$  and found that this material demonstrated high thermal stability, basicity, and recyclability as a catalytic material during transesterification of waste cooking oil to biodiesel.

Several reports had been published mobilizing the global community on renewable energy resources such as biodiesel to alleviate the escalated energy needs of the public and stem the environmental contaminant effects of tapping fossil fuel energy from coal, natural gas and petroleum crude

oil. In broad terms, biofuels have four underlying impelling cost-effective forces including energy independence for nations [15], remediation of climate change, economic development, hedging, among others. Utilizing biodiesel as fuel for generating energy produces small levels of greenhouse gases (GHGs), contributing minimally to global warming and climate change [15,16]. Therefore, the environment is more protected when renewable fuels such as biodiesel is used for energy production. For this reason, much interest had focussed on biodiesel fuels as alternative and ecologically desirable replacements for petrodiesel fuels. Biodiesel has been begun to develop in preference to fossil fuel conventional diesel including renewability, biodegradability, ready-to-use accessibility [18], portability, reduced sulfur profile and aromatic content, greater effectiveness, greater cetane number, safer handling and preferred emission characteristics [19]. At the same time, the high costs of biodiesel production have been identified, thereby affecting full commercialization of its production and wide applicability of the biodiesel in the sub-Saharan continent [20].

The manufacturing cost of biodiesel from the feedstock view has recently inspired researchers to gain insight into eco-friendly applications of waste catalysts as a substitute for their standard non-waste catalyst currently used in the production of biodiesel. Moreover, as part of a currently proposed future work in our laboratory, the synthesis of solid base catalysts such as hydroxy sodalite was undertaken for study for its plausible and probable industrial exploitation in biofuels besides limited information available in the literature in this direction. One of the ways of accomplishing this is the green method of catalytic synthesis of waste-derived catalysts (e.g. HSOD) from coal combustion waste CFA and WIB in a batch reactor to replace those that are not environmental friendly and cost-effective. At the moment, majority of the literature reports on biodiesel synthesis using solid catalysts focus on batch processes [21], but the catalysts used for the production were not synthesized using sustainable technology based on source of feedstock (as waste). Therefore, one of the current research efforts is being stimulated to investigate a solid base-catalyzed transesterification reaction utilizing the waste-derived catalyst in a continuous operation in a fixed bed reactor via this catalytic performance study.

Waste cooking oils are being disposed into the environment in South Africa and most other sub-continental Saharan states from major restaurants, hotels, canteens to a high tonnage. South Africa alone accounts for about 28 million tons annually. Only 2-3 million tons are converted to batch system biodiesel production. Interestingly, 26/25 million tons of the WCO are unutilized [22]. The management of the intensively generated waste cooking oil (WCO) from homes, restaurants, groceries and renderers/abattoirs respectively are viewed as a robust option by researchers to elevate biodiesel production to an eco-innovation, that is creating opportunities whereby economic growth through biodiesel production process technologies is sustainable with a value chain integrated in the biodiesel

industry and related product within the sub-Saharan African zone.

This study, in addition to alleviating the effect of the negative environmental impact of the CFA, WIB and WCO wastes, employs the use of waste materials to synthesize solid hydroxy sodalite catalyst from CFA and WIB. It also evaluates the catalytic efficiency in transesterifying waste cooking oil (WCO) to biodiesel of the waste-derived catalyst and the non-waste synthetic hydroxy sodalite. The general catalyst synthesis is therefore eco friendly; offering a sustainable structure for the production of commercial biodiesel in the Sub-Saharan area.

## 2. Experimental

### 2.1. Materials

The chemical reagents used in this research were purchased from Sigma-Aldrich/Merck, South Africa. Coal fly ash and waste industrial brine were collected from Mpumalanga's Tutuka power and minefield's wastewater treatment plants in South Africa, respectively. The coal fly ash was preserved as received under air-tight plastic bucket, while the waste industrial brine was preserved securely in sealed plastic bottles and refrigerated prior to experimentation in order to retain its properties. Similarly, the WCO was collected from the University of the Witwatersrand Students' Cafeteria, South Africa, and kept in a sealed plastic bottle for pre-treatment and characterizations.

In this study, two important pre-treatment steps were carried out on the feedstocks. It includes removal of ferro-magnetic materials from the Coal Fly Ash (CFA) by mechanical agitation of CFA powder sample and iron magnetic rods for about 20 minutes, and the iron magnetic materials were discarded. Secondly, the suspended particles and inorganic residues contained in the waste industrial brine (WIB) were removed by filtration. This was followed by the measurement of the salinity and pH of the WIB using the conductivity/TDS OHAUS meter model 3100 M-B instrument. The CFA powder and WIB mixture was set to the first stage-hydrothermal reaction. Heating and stirring were maintained using hotplate magnetic stirrer (H4000-HSE, Benchmark Scientific Inc. USA). The second step-hydrothermal process was performed using Parr instrument company autoclave made of stainless steel 45-mL Teflon-lined cup for crystallization of the hydrothermal synthesis product. After the hydrothermal process, hot air oven (Labcon 5016 U-Model, South Africa) fitted with top suspended thermometer (0-200 °C) was used to dry the resultant sample. Centrifugation was used to separate hydrothermal crystallization products using Roto Fix 32 A-SOP centrifuge model: Hettich, Germany. Most of the experimental set-up was supported and clamped and the biodiesel produced was evaluated qualitatively and quantitatively using Gas chromatography-Mass spectroscopy (GC-MS)-QP2010 Ultra/SE-Shimadzu Corporation, Japan.

### 2.2. Method

#### 2.2.1. Synthesis of sodalite catalyst from CFA and industrial waste brine

Hydrothermal synthesis methodology was adapted for synthesizing the waste-derived HSOD catalyst having been widely applied by researchers [20, 12,13]. A mass ratio of 1:1 CFA and NaOH in WIB solution was subjected to magnetic stirring and heating at 47 °C for 48 h at 300-500 rpm [24] ageing condition. After the removal of the iron magnetic particles, the CFA and WIB were mixed and subjected to ageing, from which a slurry was obtained. The entire mixture was transferred to an autoclave Teflon lined cup, sealed and subjected to hydrothermal treatment in a 140 °C LABCON hot air oven for crystallization of the waste-derived catalyst over a reaction time of 48 h. The crystallization product was cooled at room temperature in a running tap, the mixture was separated by centrifugation of the top clear supernatant filtrate from the solid crystal mass. The solid sample was washed with distilled water several times and the effluent filtrate pH was monitored between 10 and 11. The resulting washed solid crystalline waste-derived sample was put into a crucible and transferred to an oven at 90 °C to dry overnight. The dried sample was ground into powder using mortar and pestle and sent for calcination to an air muffle furnace at a temperature of 200 °C for 2 h before characterization and utilization for transesterification.

#### 2.2.2. Synthesis of non-waste reference HSOD catalyst

Non-waste hydroxy sodalite catalyst was synthesized and used as a reference. The catalyst was synthesized as described by [14].

#### 2.2.3. Characterization of catalysts produced

Crystalline and phase changes in the powder samples were tested using the German diffractometer D2 PHASER Bruker X-ray with Cu K $\alpha$  radiation. The elemental composition of the powder CFA sample was carried out by using X-ray fluorescence (XRF), Energy dispersive X-ray (EDX) method. A micromeritic Tri-Star 3000 surface area and porosity analyzer were used to achieve surface area, pore size and volume of the catalysts. At 77 K, the experiment produced nitrogen adsorption-desorption isotherms via the technique of Brunauer-Emmett-Teller (BET).

The characterization method of Fourier Transform Infrared (FT-IR) was used to acquire the chemical functional groups of coal fly ash and synthesis products such as waste catalyst, non-waste HSOD catalyst and biodiesel produced. Spectra were acquired from a Perkin Elmer 100 FTIR Spectrometer in the range 4000-450 cm<sup>-1</sup> in a transmittance mode. Fifty milligrams of the sample were placed on the Diamond Attenuated Total Reflectance (ATR) device accessory positioned on the device holder using the sample turning bottom before the spectrum could be generated.

Electron scanning microscopy (SEM) provides data about the basic constituent elements of coal fly ash and the catalyst synthesized. For each sample in a Carl Zeiss Sigma FESEM Oxford X-ACT EDX detector operating at an acceleration voltage of 5.00kV, a thin layer of powder

sample was mounted on sample carbon-tapped studs and an air duster used to blow away excess powder. Double gold-palladium (AuPd) coating was applied.

### 2.3. WCO physical and chemical characteristics

WCO is available in huge tonnage in South Africa [22], and was employed for the batch transesterification experiments. It was filtered for solid and other contaminants to be removed. Prior to a transesterification process, acid value, density, free fatty acid (FFA) content, etc., were determined. The physicochemical properties of the feedstocking material such as iodine value, saponification value and viscosity were also evaluated. This could establish the suitability of use of a heterogeneous catalyst to catalyze a high free fatty acid content oil stock in biodiesel production, and its degree of tolerance [12].

WCO's free fatty acid content was assessed and determined using Equation (1) as outlined by [12]:

$$\% \text{ FFA} = \frac{[(V - b) \times 28.2N]}{W} \quad (1)$$

where % FFA is a proportion of free fatty acid in a sample of waste cooking oil ; V is the titrant value (ml); b the volume of blank sample (ml); N a titration solution concentration (mg), and W weight of a milliliter of waste cooking oil sample. Detailed procedures are available in [22-24], respectively, for determination of iodine value (IV), acid value (AV) and peroxide value (PV). Viscosities of raw WCO and its biodiesel were measured using VISCO-88 viscometer, Malvern Instruments Inc. and determined at 40 °C according to [27]. Saponification index was checked according to [28].

### 2.4. WCO Transesterification into biodiesel.

The synthesized waste catalyst and the non-waste HSOD catalyst have been used to transesterify waste cooking oil to biodiesel. Figure 1 shows the experimental schematic. The parameters used to analyze biodiesel output conditions as illustrated by Figure 1 are methanol-to-waste cooking oil molar ratio of 15:1[26-28], catalyst amount 3 weight percent (with respect to WCO) [30], reaction time 8h, reaction temperature 60 °C [31], agitation speed 300-500 rpm [31,32]. 4 g of oil was poured into the batch reactor inside which a magnetic rod was contained. The waste cooking oil was heated to 110 °C to expel air and vaporize moisture [34].

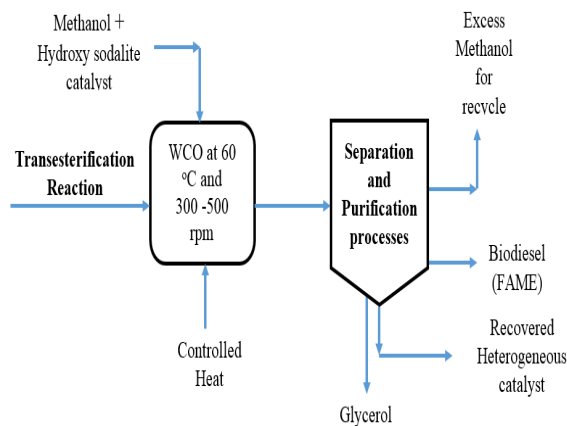


Figure 1: Schematic representation of a batch transesterification

The heated sample was left to cool down to 60 °C prior to the introduction of the feedstock and the methanol into the batch reactor. The start time, speed of rotation of the stirrer for 8 h of the reaction time as shown in Figure 1 was recorded. At the end of transesterification, the product of the reaction was obtained using a 500-ml Pyrex glass (England-BS 2021) separating funnel. It was dried in an air oven evaporator for complete methanol removal. Further, a centrifuge (Roto Fix 32A-SOP, Hettich) was used to concentrate the product mixture and then, it was possible to decant the biodiesel from the solid catalyst and glycerol mixture. The recovered solid catalyst and the glycerol were preserved, while fatty methyl ester (FAME) (biodiesel) was collected for further analysis.

Further, the solid sodalite catalysts (waste derived hydroxy sodalite and non-waste hydroxy sodalite), methanol from the transesterification reaction mixture were recovered. Finally, the yield of biodiesel was calculated using Equation (2) [32,33]:

$$\% \text{ Yield of Biodiesel} = \frac{\text{Mass of biodiesel Production}}{\text{Mass of waste cooking oil used}} \times \frac{100}{1} \quad (2)$$

#### 2.4.1. Sample injection and analysis

Prior to injection of the biodiesel for analysis, a milliliter of reaction product sample was collected and made up with hexane to a 100 mL solution and filtered using microporous membrane before analyzed by GC-MS. Helium (He) as the carrier gas was set at a flow rate of 1.5 ml min<sup>-1</sup>, and the column (30 m x 0.32 mm x 0.25 μm) temperature was in the range 120-300 °C at the rate of 10 °C min<sup>-1</sup>. Flame ionization detector (FID) was installed. The injector/detector interface temperature was in the range 250 °C, while the sample volume in a splitless mode was 1.0 μL. The MS was set to scan in the range of 35-550 m/z. The WCO conversion was calculated as reported by [36] using Equation (3) :

$$\% \text{ Conversion} = \frac{M_{\text{ester}}}{3X \frac{M_{\text{oil}}}{MW_{\text{oil}}} MW_{\text{ester}}} \times \frac{100}{1} \quad (3)$$

where  $M_{\text{ester}}$  is the obtained ester (g),  $M_{\text{oil}}$  is WCO mass used (g), and  $MW_{\text{oil}}$  is the average molecular mass ( $\text{gmol}^{-1}$ ) of WCO. The results obtained agreed with similar studies in the literature [28,29].

### 3. Results and Discussions

**Table 1:** Physical and chemical properties of waste cooking oils in the literature compared to those obtained in the current study.

#### 3.1. WCO chemical and physical characteristics

Table 1 shows the physicochemical properties of WCO used in this study compared to those in the literature. Derivatives of vegetable oils have been found to be one of the sustainable ways of alternative source of energy widely spreading and gaining acceptance [12]. However, the direct use of WCO and other vegetable oils as fuel for internal combustion engines is only possible through transesterification processes that reduce the viscosity and FFA content of triglycerides as shown in Table 1.

Property	Ref. [35]	Ref. [36]	Ref. [13]	Ref. [37]	This study
	Value				
Palmitic acid (wt. %)	-	8.5	-	34.80	36.64
Stearic acid (wt. %)	-	3.1	-	7.90	2.05
Oleic acid (wt. %)	-	21.2	-	53.30	45.10
Linoleic acid (wt. %)	-	55.2	-	4.00	0.17
Linolenic acid (wt. %)	-	5.9	-	-	1.63
Others (wt. %)	-	4.2	-	-	14.41
Water/moisture (wt. %)	0.12	1.9	< 0.05	0.20	-
Density ( $\text{gcm}^{-3}$ )	0.926	0.91	0.87	0.91	0.778
Kinematic viscosity ( $\text{mm}^2\text{s}^{-1}$ )	40.2	4.2	-	4.54	82.62
Flash point ( $^{\circ}\text{C}$ )	286	-	-	-	-
Pour point ( $^{\circ}\text{C}$ )	-15	-	-	-	-
Saponification value ( $\text{mg KOH g}^{-1}$ )	193.2	207	-	194.40	191.48
Acid value ( $\text{mg KOH g}^{-1}$ )	2.1	3.6	-	3.75	4.94
Free fatty acid (% FFA)	-	-	-	-	2.48
Iodine value ( $\text{gI}^2 100\text{g}^{-1}$ )	108	83	-	-	-
Sulphur ( $\text{mg Kg}^{-1}$ )	5	-	-	-	-
Sodium ( $\text{mg Kg}^{-1}$ )	-	6.9	-	-	-

Carbon residue (% wt wt <sup>-1</sup> )	0.18		-	-	-
Peroxide Value (Meq Kg <sup>-1</sup> )	-	23.1	-	-	0.035
Average Molecular weight (g Mole <sup>-1</sup> )	-	-	-	-	878.94
Melting point (°C)	-	-	30	-	-
High heating value (MJ)	-	-	40	-	-

**Table 2:** Major elements of raw fly ash

									Remarks
Element	Ti	Fe	Al	Si	Mn	Ca	K	P	Si : Al
% Amount	1.84	2.75	29.37	54.15	0.38	3.67	7.85	0.002	1.84

**Table 3:** Major oxides of raw fly ash

												Remarks
CFA major oxides	SiO <sub>2</sub>	Al <sub>2</sub> O <sub>3</sub>	FeO/ Fe <sub>2</sub> O <sub>3</sub>	MnO	MgO	CaO	Na <sub>2</sub> O	K <sub>2</sub> O	P <sub>2</sub> O <sub>5</sub>	TiO <sub>2</sub>	SO <sub>3</sub>	CFA Class
% Mass	57.9	31.12	2.65/ 0.33	0.04	0.95	4.28	0.13	0.66	0.39	1.52	-	F

**Table 4:** Minor elements of raw fly ash

Element	Co	Cr	Cu	Nb	Ni	Rb	Sc	Sr	U	V	Zr	Zn
% Amount	7.13	10.9	2.59	0	1.08	1.60	6.06	39.56	0.44	7.73	20.19	2.72

**Table 5:** Major elements of synthesized waste-derived hydroxy sodalite catalyst

Element	Ti	Fe	Al	Si	Mn	Ca	K	P	Remarks
% Amount	1.98	2.96	31.62	58.29	0.44	3.95	0.76	0.00	Si/Al 1.84

**Table 6:** Minor elements of synthesized waste-derived hydroxy sodalite catalyst

Element	Ba	Co	Cr	Cu	Nb	Ni	Rb	Sc	Sr	U	V	Zr	Zn
% Amount	0.001	0	10.18	3.30	0.0002	0	0.508	2.65	47.92	0.88	6.46	22.18	5.92

**Table 7:** BET analysis of waste-derived hydroxyl Sodalite Catalyst

Sample	Surface area (m <sup>2</sup> /g)	Pore volume (cm <sup>3</sup> /g)	Pore size (nm)	References
non-waste derived HSOD [at 140 °C]	0.1645	0.0013	30.9192	[16]
Waste-derived HSOD [at 140 °C]	33.0450	0.1320	16.2292	This study

**Table 8:** EDX Analysis of Raw CFA and Waste-derived HSOD

Coal fly ash (CFA)			Waste-derived HSOD		
Element	Wt %	Atomic %	Element	Wt %	Atomic %
C	7.45	12.38	C	21.01	30.14
O	42.96	53.62	O	44.48	47.92
Mg	0.48	0.39	Na	8.18	6.13
Al	19.01	14.07	Al	9.69	6.19
Si	23.60	16.78	Si	13.73	8.43
Ca	2.66	1.33	Ca	1.98	0.85
Ti	1.17	0.49	Ti	0.93	0.33
Fe	2.67	0.95	-	-	-
Total	100.00			100.00	

**Table 9:** Percentage biodiesel yield during transesterification

S/N	Synthesis Catalyst	Amount of Catalyst (wt. %)	MeOH: WCO	Temp. (°C)	Reaction Time (h)	Stirring Speed (RPM)	Biodiesel Yield (%)
1	NWR HSOD	3	15:1	60	8	500	85.0
2	WD HSOD	3	15:1	60	8	500	89.4

NWR: Non-Waste Reference; WD: Waste Derived; HSOD: Hydroxy Sodalite, RPM: Revolution per minute

### 3.2. Synthesis and characterization of waste-derived hydroxy sodalite

In this study, hydrothermal synthesis methodology was adopted in view of its operational efficiency in preparing bulk metal catalysts for high purity, cost-competitiveness and easy control of operating variables such as temperature and reaction time [11].

### 3.3. X-ray Fluorescence (XRF) Analysis

Raw XRF data give quantitative and qualitative information on the presence of elements and compounds of interest detected by the instrument as presented in Table 2 to Table 6. Table 2 shows the XRF compositional elements present in the CFA used in this study with 29.37 and 54.15 per cent aluminum and silicon, respectively. They are the major raw materials of interest in the CFA for synthesis of waste-derived hydroxy sodalite (waste-derived HSOD). It was observed that in addition to being 83.52 % of the CFA by mass, Si / Al ratio was found to be 1.84. This value is critical during the structural buildup of crystallization. The structural composition of a formed zeolite also is restricted [41], and this author believes that adjusting the Si/Al ratio during the synthesis of catalysts may cause an undesirable phase in the final crystalline. The implication is that the formation of a particular zeolite species is dependent on the ratio of Si / Al in the raw material [42]. It is evident that formation of 1.14 - 1.22 Si / Al ratio in the product tends to be thermally less stable. This ratio controls SiO<sub>2</sub>/Al<sub>2</sub>O<sub>3</sub> ratio on the physical properties of a zeolite [41], for example, the increase in the SiO<sub>2</sub>/Al<sub>2</sub>O<sub>3</sub> increases the acid resistance, thermal stability, hydrophobicity, whereas the affinity for polar absorbance and cation content are decreased. Similarly, the hydrophilicity and cation exchange properties were increased due to the decrease in the SiO<sub>2</sub>/Al<sub>2</sub>O<sub>3</sub> ratio.

From Table 3, the two main oxides of CFA are silica and Alumina and their percentage elemental compositions are 57.9 and 31.12 %, respectively.

According to [43], CFA with SiO<sub>2</sub>, Al<sub>2</sub>O<sub>3</sub> and FeO/Fe<sub>2</sub>O<sub>3</sub> mass compositions above 70 % is regarded as a class F, and from the results obtained in this study, the South African CFA is therefore confirmed as a typical class F CFA. Similarly, the XRF results of Table 4 presents the minor elements of CFA which are deemed as impurities by the instrument, while Table 5 shows the elements which have similar content as that of Table 2. This observation explains the adequacy of precursors required for synthesizing the desired waste-derived hydroxy sodalite catalyst. Table 6 indicates the impurities which are usually found in the synthesized waste-derived HSOD catalyst and most times, they appear as trace elements.

### 3.4. Fourier transform infrared (FT-IR) analysis

The spectroscopy of Fourier transform infrared (FT-IR) was used to analyze the chemical functionality of raw CFA powder, the catalyst HSOD derived from waste and reference hydroxy sodalite (non-waste HSOD). In this case, biodiesel produced at two different experimental conditions using the synthesized catalysts were analyzed employing the FT-IR analytic technique. The result of the analysis is presented in Figure 2. The three FT-IR spectral patterns depicted in Figure 2, reveal the chemical transformations occurring during the conversion of raw CFA to the zeolitic waste-derived hydroxy sodalite. Due to the SiO<sub>5</sub> Sillimanite phase (Al<sub>1.98</sub>Fe<sub>0.03</sub>), the characteristic fingerprint region of the raw CFA spectra (1222-452 cm<sup>-1</sup>) may be assigned to the compositional materials of the source raw coal fly ash. SiO<sub>5</sub>

is a pentacoordinate silicon (IV) complexes associated with the framework of Sillimanite [44].

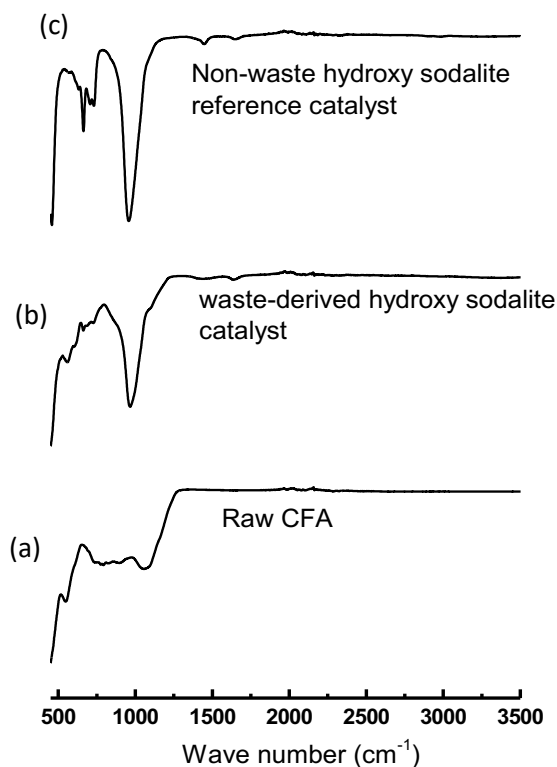


Figure 2: (a) FT-IR Spectra-Raw CFA, (b) waste-derived hydroxy sodalite catalyst and (c) waste-free hydroxy sodalite reference catalyst.

This is in perfect agreement with the XRD result (JCPDS file no. -084-0983). Invariably, the XRD results (JCPDS file no. 031-1271 and JCPDS file no.081-0599) are respectively assignable to the waste-derived HSOD and non-waste HSOD reference catalysts. The peak shown at  $\sim 500\text{ cm}^{-1}$  characterizes the Al-O-Si and Si-O-Si bending vibrations. The distinctive peaks at  $680\text{ cm}^{-1}$  and  $750\text{ cm}^{-1}$  are due to the (Si, Al)-O-(Si, Al) [14] symmetric stretching. Also, the wide peak at  $1000\text{ cm}^{-1}$  can be ascribed to the (Si, Al)-O-(Si, Al) asymmetric transmission stretch agreed with the literature [13, 42, 43].

### 3.5. Textural Analysis

Table 7 presents the BET-N<sub>2</sub> evaluation of the waste-derived HSOD produced from CFA and WIB to determine the textural characteristics of the waste-derived HSOD catalyst. The table demonstrates that, compared to the waste-derived HSOD catalyst ( $33.05\text{ m}^2\text{g}^{-1}$ ) as obtained in this research, the non-waste reference HSOD has a very small specific surface area.

In a related study [47], a BET-N<sub>2</sub> specific surface area of  $9.7\text{ m}^2\text{g}^{-1}$  was achieved using deionized water as solvent for zeolitic sodalite from coal fly ash in a hydrothermal-sol-gel method. Similarly, in ref [48] used a class F fly ash from the Stolwa Wola SA heat power plant, Poland to perform a sequence of reactions for zeolite

preparations. Result of the NaOH-CFA treatments showed that a 90 weight percent diffractometry highest sodalite formed was analyzed texturally and a BET surface area of  $33\text{ m}^2\text{g}^{-1}$  was obtained and this agrees with the surface area of  $33.0450\text{ m}^2\text{g}^{-1}$  obtained from this study. Therefore, it can be expected that the waste-derived HSOD catalyst would be catalytically better in transesterification reactions due to the enhanced accessible reaction active sites and attachment openings achieved in this study [40].

Figure 3(a) and Figure 3 (b) display the N<sub>2</sub> adsorption-desorption isotherm of the waste-derived HSOD and the particle size distribution (PSD) based on the BET instrument set conditions at  $-196.15\text{ }^\circ\text{C}$ . Figure 3 (a) reveals that the waste-derived HSOD has a typical IUPAC type IV isotherm implying a mesoporous material [49].

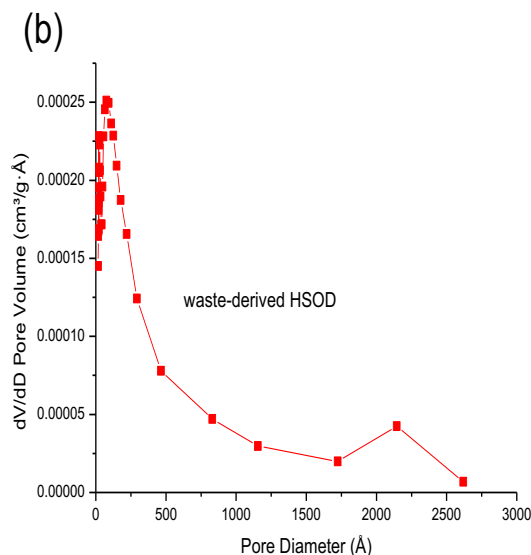


Figure 3(a) and Figure 3(b): BET surface area isotherm and BJH particle distribution for synthesized waste-derived HSOD using CFA and WIB

As can be seen, the isotherm exhibits adsorption steps from  $PP_0^{-1} = 0.13$  to  $1.0$  with capillary condensation mesoporic region  $0.86\text{ PP}_0^{-1}$  to  $0.99\text{ PP}_0^{-1}$ , where N<sub>2</sub> uptake is



significant. In order to gain insight into the texture and shape of the mesoporous material adsorption hystereses, the IUPAC classification is given in the literature [50]. [51] correlates the shape and the textural properties of the waste-derived HSOD depicted in Figure 3(b) using the BJH adsorption branch for mesopores [52]. The adsorbed sample has both micropore and mesopore particle size distributions. This shows a primary maximum at a pore size of around 20 Å or 2 nm and a secondary maximum at a pore size of 21.5 Å or 2.15 nm. The PSD of the studied waste-derived HSOD typically indicates the particle size grading as consisting of a narrow micropores of up to 2.0 nm and 2.0-2.15 nm mesopores. The predominance of sodalite mesopores, therefore, is in the range 2.0-2.15 nm.

### 3.6. X-Ray Diffraction

D2 PHASER Bruker X-ray was used to study the diffraction patterns and the crystalline nature of the powder samples.

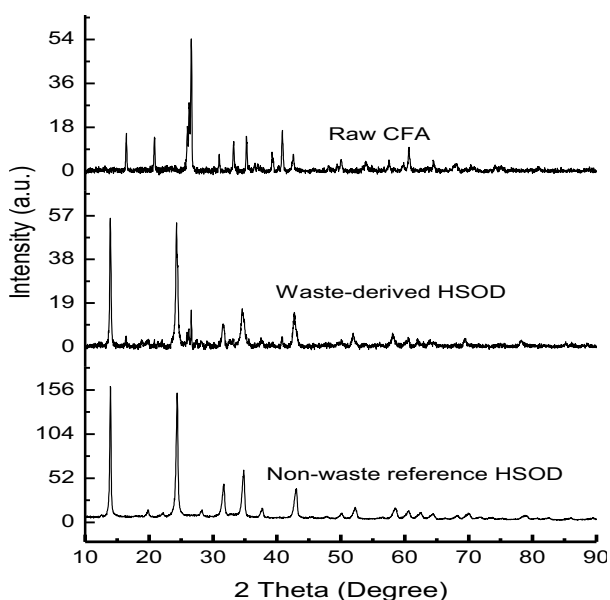


Figure 4: XRD pattern for waste-derived HSOD and non-waste reference HSOD catalyst synthesized at 140 °C

Figure 4 shows the presence of sillimanite  $[(Al_{1.98}Fe_{0.02})SiO_5]$ , JCPDS file no. 084-0983] in the raw CFA. The result was expected due to the pretreatment of the CFA which significantly depleted the iron magnetic impurities to a negligible amount in the feedstock. It should be recalled that during feedstock pre-treatment, the iron particles in the CFA were removed and the essence was to reduce reaction complex during ageing process. The removal also favored silicon/aluminium ratio which is very essential to hydrothermal crystallization of the desired zeolitic waste-derived HSOD catalyst.

The major characteristic crystalline phases identified on the  $2\theta$  detector position are 11, 33 (major peak), 35, 46 and 62 (Figure 4). Iron particles removed from the CFA during pretreatment might not only enhance mass transfer activity during ageing mixing and hydrothermal treatment processes but drastically reduce the degree of impurity in the final synthesis product. XRD diffractograms

of waste-derived HSOD catalyst show pure crystalline phase of HSOD  $[(1.08Na_2O \cdot Al_2O_3 \cdot 1.68SiO_2 \cdot 1.8H_2O)]$ , JCPDS file no. 031-1271] with major peaks at 8, 24.5 (major peak), 33.5, 35.2, 43.5, 52 and 58°  $2\theta$  scan (Figure 4). On the other hand, the crystalline phase depicted by the non-waste HSOD reference catalyst indicates a composition of  $[Na_{5.44}Br_{0.26}(AlSiO_4)_6(H_2O)_4]$  sodalite (Na, Br) sodium bromide aluminium silicate hydrate; JCPDS file no. 081-0599] with 8, 24.5 (major peak), 31.5, 34.5 and 42.7°  $2\theta$  scan.

### 3.7. Morphology and elemental composition

The FESEM detector (Oxford X-ACT EDX) was used to obtain the raw CFA SEM micrographs and the hydrothermal synthesis products described in Figure 5. Raw CFA-SEM image shows spherically fine but smooth surface hollow cenospheres of various sizes and non-crystalline glass beads [12-39]. Class F CFA feedstock typically comprises of alumino-silicate glass, crystalline mullite, hematite/magnetite iron oxides, quartz and unburned carbon. However, a few desulfurizing flue gas products, some tiny quantities of gypsum, calcite and calcium may be present [53]. These constitute the various microspheres of individual intergrowths or grains and shapes which are generally porous. The SEM images of the waste-derived and non-waste reference HSOD show absence of the spherical particles observed of the CFA. In the case of the waste-derived HSOD, this absence of the spherical particles shows that there has been efficient conversion of the CFA and WIB to zeolitic waste-derived sodalite under the hydrothermal reaction conditions [45-37].

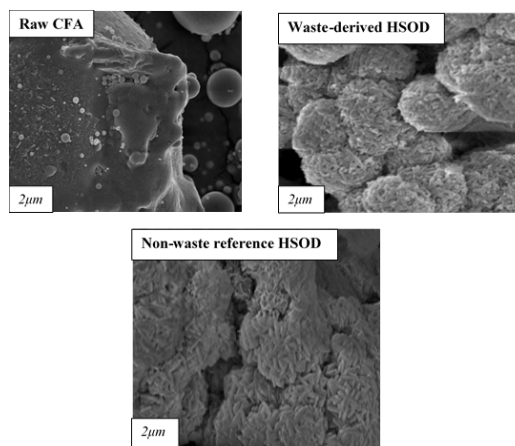


Figure 5: SEM images of raw CFA, waste-derived HSOD and non-waste reference HSOD

The sodalite particle surface is rough therad-like balls that reveal the formation of crystals during hydrothermal treatment. These crystallites are tiny ( $< 1\text{ mm}$  in size) and cause fast nucleation at the expense of impurities mentioned previously in the precursor [56]. In addition, presence of these amorphous SEM images of the raw CFA sample is thought to be due to heating and cooling regimes of the CFA during coal combustion in the power plants [24]. Table 8, displays the EDX of the raw CFA and the waste-derived HSOD. The table indicates presence of  $O > Si > Al > C > Fe > Ca > Ti > Mg$  in decreasing order of elemental magnitude.

Presence of carbon could be as a result of unburned carbon [52] at the coal boiler or as a result of inherent carbon in the carbon tape used during sample preparation. It is observed that the EDX of the waste-derived HSOD shows constituent of  $O > C > Si > Al > Na > Ca > Ti$  in decreasing order of abundance. Oxygen is essential in the silicate aluminate composition for sodalite synthesis. The presence of carbon in the EDX result for the waste HSOD is as mentioned due to the carbon taped stud for sample preparation. The absence of iron (Fe) in the EDX of the synthesized waste HSOD was due to the initial Ferro-magnetic removal treatment on as-received CFA prior to hydrothermal process. From the EDX result, the calculated Si/Al ratio of 1.24 was obtained and this value is essential for hydrothermal transformation of CFA and WIB to HSOD. During hydrothermal synthesis of zeolitic HSOD, Si/Al ratio has been revealed to be in the range of 1.0 to 1.5 [15-39].

### 3.8. Waste cooking oil Transesterification to biodiesel

The catalyst activity of the HSOD catalyst derived from waste and the non-waste referral catalyst was evaluated under a methanol-to-oil ratio of 15:1, a catalyst of three weight percent with a stirring speed of 300-500 rpm, a reaction temperature of 60 °C and a reaction time of 8 h. Details of percent biodiesel output are shown in Table 9 after the transesterification reactions.

The quality and quantity of biodiesel product were evaluated using a GC-MS QP2010. Figure 6 shows the FT-IR result for the biodiesel product samples of the transesterification of the WCO catalyzed by the waste-derived HSOD and non-waste reference HSOD solid base catalysts synthesized at 140 °C.

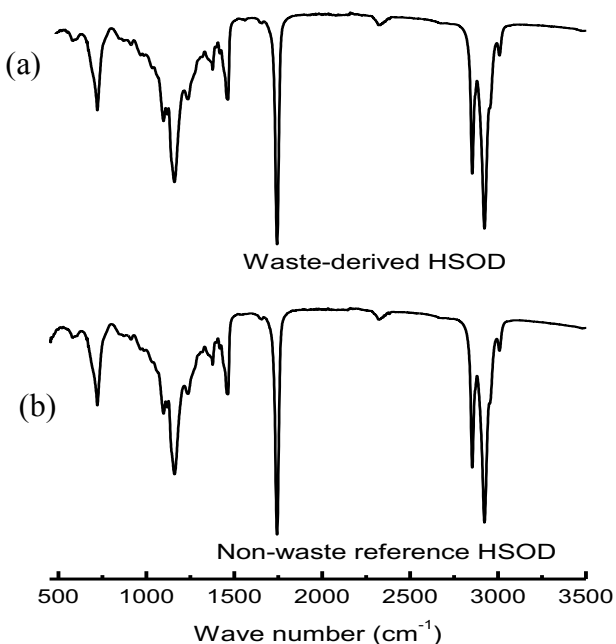


Figure 6: (a) FT-IR HSOD biodiesel derived from waste and (b) HSOD biodiesel produced from non-waste samples

The spectral patterns show that biodiesel was produced. The spectra peaks of 4000-1500  $cm^{-1}$  in the functional group are 2924, 2854, 2317 and 1744  $cm^{-1}$ , 2924 and 2854  $cm^{-1}$  are connected with bending vibrations of alkyl methylene or  $-CH_2-$  stretches. The strong peak present at 1743  $cm^{-1}$  is attributed to the presence of  $C=O$  stretching vibration of carbonyl groups in the triglycerides, while the peaks present in the region of 1120-1090  $cm^{-1}$  reflects the stretching vibration of  $C=O$  ester [57]. Accordingly, 2924 and 2854  $cm^{-1}$  are associated with bending vibrations of alkyl methylene or  $-CH_2-$  stretches due to  $C=O$  ester indication at 1744  $cm^{-1}$  [12]. It is observed that at 2317  $cm^{-1}$ , weak stretches of vibrations assignable to  $-C \equiv C-$  triple bonds occur. In the fingerprint region of the spectrum 1500-400  $cm^{-1}$ , it can also be observed that mandatory characteristic  $-CH_2-$  stretches associated with alkyl methylene at 1459  $cm^{-1}$  depicts the characteristic fatty acid methyl ester. The 1378  $cm^{-1}$  is attributed to the methyl alkyl stretches [14]. The spectra have characteristic peaks associated with tertiary alcohol at 1159  $cm^{-1}$ . The rocking stretches assignable to  $-CH_2-$  or mono-substituted benzene show strong peak at 721  $cm^{-1}$ .

It can be seen from Figures 7 and 8 that the viscosities of the WCO and the produced biodiesel are 82.62  $mm^2s^{-1}$  and 46.14  $mm^2s^{-1}$  respectively. This implies that the viscosity of WCO has been reduced drastically by transesterification process for application in internal combustion engines as fuel.

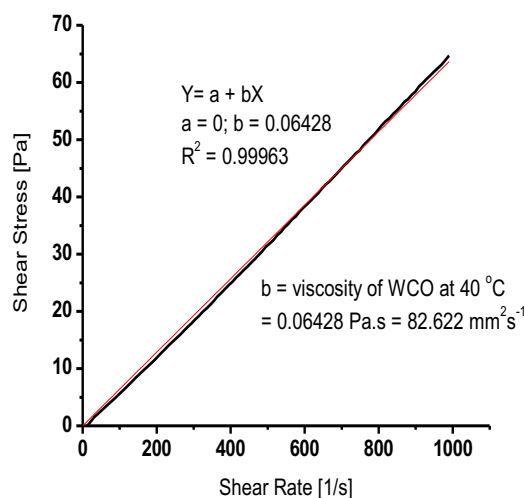
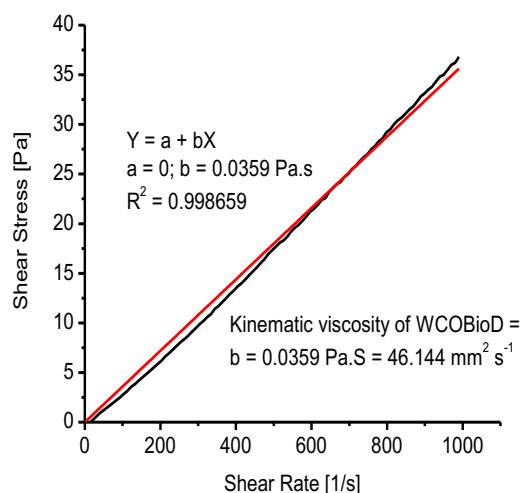


Figure 7: Rheological determination of the kinematic viscosity of waste cooking oil at 40 °C.



**Figure 8:** Kinematic viscosity of WCO biodiesel at 40 °C

**Figure 9:** Catalytic conversion of WCO to biodiesel using non-waste reference and waste-derived HSOD catalysts.

From the results (Table 9), it can be stated that biodiesel yield using the waste-derived HSOD catalyst for WCO transesterification is higher than that of the non-waste reference catalyst. It is observed that the non-waste HSOD and waste-derived HSOD yielded 85.0 and 89.4 % biodiesel respectively after an 8 h transesterification reaction at 97 % feed conversion (Figure 9). The exceedingly higher performance of the waste-derived HSOD catalyst can be attributed to improved surface area of catalyst compared to the non-waste HSOD reference catalyst. A high specific surface area is associated with larger number of active sites available in the catalyst framework indicating a potentially higher catalytic activity for the waste-derived catalyst [40]. In a similar transesterification reaction, waste-derived CaO from snail shell has been used to achieve 98 % biodiesel yield at room temperature using soybean oil. It was

established that the successful result [58] was due to enhanced BET surface area (2.7-7.0 m<sup>2</sup> g<sup>-1</sup>) of the derived heterogeneous catalyst when compared with the catalytic performance of a commercial CaO catalyst's BET surface area (1.0 m<sup>2</sup>g<sup>-1</sup>) for soybean oil transesterification reported by [59]. In a transesterification process using soybean oil on a catalyst loading 5.8 weight percent after a 9 h reaction time, the CaO catalyst obtained from eggshells was used to achieve a 96 percent biodiesel yield [60]. The GC-MS analysis indicate the formation of fatty acid methyl esters (FAMES) which was compared with a commercial biodiesel standard according to American Society for Testing and Materials (ASTM) and European Union (EU) norms on commercial biodiesel standard.

#### 4. Conclusions

The synthesis of pure and high surface area waste-derived HSOD catalyst for transesterification of Waste Cooking Oil (WCO) to biodiesel was studied using CFA and WIB as feedstock. The experimental process conditions employed were the two-step hydrothermal synthesis reported by [23].

The following conclusions emanated from the study:

- The result revealed that the South African CFA used for the study is a class F CFA.
- Si/Al ratio of 1.24 is necessary for hydrothermal transformation of the CFA and WIB into HSOD.
- The synthesized waste-derived HSOD has a surface area of 33.05 m<sup>2</sup>g<sup>-1</sup>; a significant enhancement in the specific surface when compared to results found in the literature, and it implies increased catalytic performance and more biodiesel production due to the increased catalytic surface area.
- An invaluable precursors (e.g. CFA & WIB) employed for catalyst synthesis that provide sustainable waste-to-wealth development in South Africa and the Sub-Saharan zone were identified, thus; opening a new window for R&D in the field of environmental engineering, heterogeneous catalysis, bioprocessing, bio-resource control and waste recovery.

#### Acknowledgements

Mr Phalli Caleb Motlatsi, School of Chemical and Metallurgical Engineering, Wits, is acknowledged for his technical expertise and assistance in the GC analysis of the reaction mixtures.

#### References

- [1] O. Babajide, L. Petrik, N. Musyoka, B. Amigun, and F. Ameer, "Use of coal fly ash as a catalyst in the production of biodiesel, *Petroleum and Coal*, Vol. 52, no. 4, pp. 261-272. Oct. 2010.
- [2] A. E. Özdemir and S. Akkaya Oy, "Alternative renewable energy producing systems by utilizing piezoelectric transducers," in *2016 IEEE International*

- Conference on Renewable Energy Research and Applications (ICRERA)*, 2016, pp. 59–62.
- [3] A. Harrouz, M. Abbes, I. Colak, and K. Kayisli, “Smart grid and renewable energy in Algeria,” in *2017 IEEE 6th International Conference on Renewable Energy Research and Applications (ICRERA)*, 2017, pp. 1166–1171.
- [4] C. Gunathilake, I. W. Kularathne, A. C. Rathneweera, C. S. Kalpage, and S. Rajapakshe, “The effect of use of biofuels on environmental pollution - A Review,” *Int. J. Renew. Energy Res. IJRER*, vol. 9, no. 3, pp. 1355–1367, Sep. 2019.
- [5] M. W. Gitari, L. F. Petrik, and N. M. Musyoka, “Hydrothermal Conversion of South African Coal Fly Ash into Pure Phase Zeolite Na-P1,” InTechOpen Croatia, 2016, Ch. 2. (Book Chapter).
- [6] A. GreenPeace, “Greenpeace confronts ESKOM-End coal addiction and embrace renewable energy,” *ethical living*, South Africa, 2011.
- [7] H. I. Bulbul, M. Colak, A. Colak, and S. Bulbul, “Special session 1: Public awareness and education for renewable energy and systems,” in *2017 IEEE 6th International Conference on Renewable Energy Research and Applications (ICRERA)*, 2017, pp. 12–12.
- [8] A. Molina and C. Poole, “A comparative study using two methods to produce zeolites from fly ash,” *Miner. Eng.*, vol. 17, no. 2, pp. 167–173, Feb. 2004.
- [9] Y. Yaping, Z. Xiaoqiang, Q. Weilan, and W. Mingwen, “Synthesis of pure zeolites from supersaturated silicon and aluminum alkali extracts from fused coal fly ash,” *Fuel*, vol. 87, no. 10, pp. 1880–1886, Aug. 2008.
- [10] U. S. E.P.A, “Using Coal Ash in Highway Construction: A Guide to Benefits and Impacts,” 2005.
- [11] N. M. Musyoka, L. F. Petrik, G. Balfour, W. M. Gitari, and E. Hums, “Synthesis of hydroxy sodalite from coal fly ash using waste industrial brine solution,” *J. Environ. Sci. Health Part A*, vol. 46, no. 14, pp. 1699–1707, Dec. 2011.
- [12] M. O. Daramola, D. Nkazi, and K. Mtshali, “Synthesis and Evaluation of Catalytic Activity of Calcined Sodium Silicate for Transesterification of Waste Cooking Oil to Biodiesel,” *Int. J. Renew. Energy Res. IJRER*, vol. 5, no. 2, pp. 517–523, Jun. 2015.
- [13] S. Hwa Teo, Y. Hin Taufiq-Yap, U. Rashid, and A. Islam, “Hydrothermal effect on synthesis, characterization and catalytic properties of calcium methoxide for biodiesel production from crude *Jatropha curcas*,” *RSC Adv.*, vol. 5, no. 6, pp. 4266–4276, 2015.
- [14] Makgaba C Precious and Daramola O Michael, “Transesterification of waste cooking oil to biodiesel over calcined hydroxy sodalite (HS) catalyst: A preliminary investigation,” in *International conference on Sustainable Energy and Environmental Engineering (SEEE 2015)*, 2015, pp. 52–56.
- [15] F. R. A. C. Baracho, R. M. A. Baracho, R. A. Bonatti, and C. H. F. Silva, “Knowledge Management in Electricity Generation Strategic Decisions: The Dawn of the Renewable Age,” in *2018 International Conference on Smart Grid (icSmartGrid)*, 2018, pp. 148–157.
- [16] K. E. Okedu, H. A. Nadabi, and A. Aziz, “Prospects of Solar Energy in Oman: Case of Oil and Gas Industries,” p. 15, 2019.
- [17] Y. Tominaga, M. Tanaka, H. Eto, Y. Mizuno, N. Matsui, and F. Kurokawa, “Design Optimization of Renewable Energy System Using EMO,” in *2018 International Conference on Smart Grid (icSmartGrid)*, 2018, pp. 258–263.
- [18] H. Selanduray and M. H. Boosroh, “Power plant optimization in a regulated environment electricity supply industry: A least cost generation approach,” in *2008 IEEE 2nd International Power and Energy Conference*, 2008, pp. 1245–1250.
- [19] A. Karmakar, S. Karmakar, and S. Mukherjee, “Properties of various plants and animals feedstocks for biodiesel production,” *Bioresour. Technol.*, vol. 101, no. 19, pp. 7201–7210, Oct. 2010.
- [20] M. Balat, “Potential alternatives to edible oils for biodiesel production – A review of current work,” *Energy Convers. Manag.*, vol. 52, no. 2, pp. 1479–1492, Feb. 2011.
- [21] Ramli Mat, Rubyatul Adawiyah Samsudin, Mahadhir Mohamed, and Anwar Johari, “Solid Catalysts and Their Application in Biodiesel Production,” *Bulletin of Chemical Reaction Engineering & Catalysis*, Vol. 7, no. 2, pp. 142 – 149, Oct. 2012.
- [22] Roy de Gouveia, “Biogreen diesel: Converting waste cooking oil into biodiesel,” *Urban Earth*, 24-Feb-2016.
- [23] G. G. Hollman, G. Steenbruggen, and M. Janssen-Jurkovičová, “A two-step process for the synthesis of zeolites from coal fly ash,” *Fuel*, vol. 78, no. 10, pp. 1225–1230, Aug. 1999.
- [24] N. M. Musyoka, L. F. Petrik, G. Balfour, W. M. Gitari, and E. Hums, “Synthesis of hydroxy sodalite from coal fly ash using waste industrial brine solution,” *J. Environ. Sci. Health Part A*, vol. 46, no. 14, pp. 1699–1707, Dec. 2011.
- [25] BS EN 14111, “Fat and oil derivatives. Fatty acid methyl esters (FAME). Determination of iodine value,” 2003.
- [26] AOCS CD 3D-63, “Sampling and analysis of commercial fats and oils; Acid Value,” 2009.
- [27] ASTM D445, “Standard Test Method for Kinematic Viscosity of Transparent and Opaque Liquids,” 2017.
- [28] ASTM D5558 - 95, “Standard Test Method for Determination of the Saponification Value of Fats and Oils,” 2017.
- [29] R. D. Saini, “Conversion of Waste Cooking Oil to Biodiesel,” *Int. J. Pet. Sci. Technol.*, vol. 11, no. 1, pp. 9–21, 2017.
- [30] N. Ngadi, L. N. Ma, H. Alias, A. Johari, R. A. Rahman, and M. Mohamad, “Production of Biodiesel from Waste Cooking Oil via Ultrasonic-Assisted Catalytic System,” *Appl. Mech. Mater.*, vol. 699, pp. 552–557, 2015.
- [31] K.-C. Ho, C.-L. Chen, P.-X. Hsiao, M.-S. Wu, C.-C. Huang, and J.-S. Chang, “Biodiesel Production from Waste Cooking Oil by Two-step Catalytic

- Conversion,” *Energy Procedia*, vol. 61, pp. 1302–1305, Jan. 2014.
- [32] M. N. Hossain, M. S. U. S. Bhuyan, Abul Hasnat Md Ashrafal Alam, and Y. C. Seo, “Biodiesel from Hydrolyzed Waste Cooking Oil Using a S-ZrO<sub>2</sub>/SBA-15 Super Acid Catalyst under Sub-Critical Conditions,” *Energies*, vol. 11, no. 2, pp. 299 (1–13), 2018.
- [33] M. Farooq, A. Ramli, and D. Subbarao, “Biodiesel production from waste cooking oil using bifunctional heterogeneous solid catalysts,” *J. Clean. Prod.*, vol. 59, pp. 131–140, Nov. 2013.
- [34] M. O. Daramola, K. Mtshali, L. Senokoane, and O. M. Fayemiwo, “Influence of operating variables on the transesterification of waste cooking oil to biodiesel over sodium silicate catalyst: A statistical approach,” *J. Taibah Univ. Sci.*, vol. 10, no. 5, pp. 675–684, Sep. 2016.
- [35] Q. Fu, C. Song, Y. Kansha, Y. Liu, M. Ishizuka, and A. Tsutsumi, “Energy saving in a biodiesel production process based on self-heat recuperation technology,” *Chem. Eng. J.*, vol. 278, pp. 556–562, Oct. 2015.
- [36] A. N. Phan and T. M. Phan, “Biodiesel production from waste cooking oils,” *Fuel*, vol. 87, no. 17, pp. 3490–3496, Dec. 2008.
- [37] Y.-P. Peng, K. T. T. Amesho, C.-E. Chen, S.-R. Jhang, F.-C. Chou, and Y.-C. Lin, “Optimization of Biodiesel Production from Waste Cooking Oil Using Waste Eggshell as a Base Catalyst under a Microwave Heating System,” *Catalysts*, vol. 8, no. 2, p. 81, Feb. 2018.
- [38] G. Anastopoulos, Y. Zannikou, S. Stournas, and S. Kalligeros, “Transesterification of Vegetable Oils with Ethanol and Characterization of the Key Fuel Properties of Ethyl Esters,” *Energies*, vol. 2, pp. 362–376, 2009.
- [39] Z. Yaakob, M. Mohammad, M. Alherbawi, Z. Alam, and K. Sopian, “Overview of the production of biodiesel from Waste cooking oil,” *Renew. Sustain. Energy Rev.*, vol. 18, pp. 184–193, Feb. 2013.
- [40] N. Y. Yahya, N. Ngadi, M. Jusoh, and N. A. A. Halim, “Characterization and parametric study of mesoporous calcium titanate catalyst for transesterification of waste cooking oil into biodiesel,” *Energy Convers. Manag.*, vol. 129, pp. 275–283, Dec. 2016.
- [41] R. Szostak, “Hydrothermal Zeolite Synthesis,” in *Molecular Sieves: Principles of Synthesis and Identification*, R. Szostak, Ed. Dordrecht: Springer Netherlands, 1989, pp. 51–132.
- [42] X. Querol, A. Alastuey, JoséL. Fernández-Turiel, and A. López-Soler, “Synthesis of zeolites by alkaline activation of ferro-aluminous fly ash,” *Fuel*, vol. 74, no. 8, pp. 1226–1231, Aug. 1995.
- [43] R. A. Kruger, “Fly ash beneficiation in South Africa: creating new opportunities in the market-place,” *Fuel*, vol. 76, no. 8, pp. 777–779, Jun. 1997.
- [44] R. Tacke, C. Burschka, B. Wagner, and R. Willeke, “Pentacoordinate Silicon Compounds with SiO<sub>5</sub> Skeletons Containing SiOH or SiOSi Groups: Derivatives of the Pentahydroxosilicate(1–) Anion [Si(OH)<sub>5</sub>]- and Its Anhydride [(HO)<sub>4</sub>Si–O–Si(OH)<sub>4</sub>]<sub>2</sub>-,” *J Am Chem Soc*, vol. 122, no. 35, pp. 8480–8485, 2000.
- [45] J. Luo, H. Zhang, and J. Yang, “Hydrothermal Synthesis of Sodalite on Alkali-Activated Coal Fly Ash for Removal of Lead Ions,” *Procedia Environ. Sci.*, vol. 31, pp. 605–614, Jan. 2016.
- [46] T. Henmi, “Synthesis of Hydroxy-Sodalite (‘Zeolite’) from Waste Coal Ash,” *Soil Sci. Plant Nutr.*, vol. 33, no. 3, pp. 517–521, Sep. 1987.
- [47] M. C. Manique, L. V. Lacerda, A. K. Alves, and C. P. Bergmann, “Biodiesel production using coal fly ash-derived sodalite as a heterogeneous catalyst,” *Fuel*, vol. 190, pp. 268–273, Feb. 2017.
- [48] W. Franus, M. Wdowin, and M. Franus, “Synthesis and characterization of zeolites prepared from industrial fly ash,” *Environ. Monit. Assess.*, vol. 186, no. 9, pp. 5721–5729, 2014.
- [49] A. E. Persson, B. J. Schoeman, J. Sterte, and J.-E. Otterstedt, “The synthesis of discrete colloidal particles of TPA-silicalite-1,” *Zeolites*, vol. 14, no. 7, pp. 557–567, Sep. 1994.
- [50] J. C. P. Broekhoff, “Mesopore Determination from Nitrogen Sorption Isotherms: Fundamentals, Scope, Limitations,” in *Studies in Surface Science and Catalysis*, vol. 3, B. Delmon, P. Grange, P. Jacobs, and G. Poncelet, Eds. Elsevier, 1979, pp. 663–684.
- [51] K. S. W. Sing, “Reporting physisorption data for gas/solid systems with special reference to the determination of surface area and porosity (Recommendations 1984),” *Pure Appl. Chem.*, vol. 57, no. 4, pp. 603–619, 1985.
- [52] S. Storck, H. Bretinger, and W. F. Maier, “Characterization of micro- and mesoporous solids by physisorption methods and pore-size analysis,” *Appl. Catal. Gen.*, vol. 174, no. 1, pp. 137–146, Nov. 1998.
- [53] A. Derkowski, “Various methods of synthesis of zeolites from fly ash as an attempt of utilization of post-combustion wastes,” *Przeglad Geol.*, vol. 49, pp. 337–338, 2001.
- [54] D. A. Fungaro, M. Bruno, and L. C. Grosche, “Adsorption and kinetic studies of methylene blue on zeolite synthesized from fly ash,” *Desalination Water Treat.*, vol. 2, no. 1–3, pp. 231–239, Feb. 2009.
- [55] J. de C. Izidoro, D. A. Fungaro, F. S. dos Santos, and S. Wang, “Characteristics of Brazilian coal fly ashes and their synthesized zeolites,” *Fuel Process. Technol.*, vol. 97, pp. 38–44, May 2012.
- [56] J. C. Jansen, H. M. Bekkum, and E. M. Flanigen, “Introduction to zeolite science and practice,” in *Studies in surface science and catalysis*, J.C. Jansen., Netherlands: Elsevier, 1991, pp. 77–136.
- [57] J. Nisar *et al.*, “Enhanced biodiesel production from Jatropa oil using calcined waste animal bones as catalyst,” *Renew. Energy*, vol. 101, pp. 111–119, Feb. 2017.
- [58] I. Bahar Laskar, K. Rajkumari, R. Gupta, S. Chatterjee, B. Paul, and L. Rokhum, “Waste snail shell derived heterogeneous catalyst for biodiesel production by the transesterification of soybean oil,” *RSC Adv.*, vol. 8, no. 36, pp. 20131–20142, 2018.

- [59] C. R. Venkat Reddy, R. Oshel, and J. G. Verkade, "Room-Temperature Conversion of Soybean Oil and Poultry Fat to Biodiesel Catalyzed by Nanocrystalline Calcium Oxides," *Energy Fuels*, vol. 20, no. 3, pp. 1310–1314, May 2006.
- [60] A. Piker, B. Tabah, N. Perkas, and A. Gedanken, "A green and low-cost room temperature biodiesel production method from waste oil using egg shells as catalyst," *Fuel*, vol. 182, pp. 34–41, Oct. 2016.